

Generalized polarizabilities and electroexcitation of the nucleon

D. Drechsel¹, S.S. Kamalov^{1*}, G. Krein², B. Pasquini¹ and L. Tiator¹

1. Institut für Kernphysik, Universität Mainz, 55099 Mainz, Germany

2. Instituto de Física Teórica, Universidade Estadual Paulista

Rua Pamplona 145, 01405-900 São Paulo, SP - Brazil

Abstract

Generalized nucleon polarizabilities for virtual photons can be defined in terms of electroproduction cross sections as function of the 4-momentum transfer Q^2 . In particular, the sum of the generalized electric and magnetic polarizabilities $\Sigma = \alpha + \beta$ and the spin polarizability γ can be expressed by virtual photon absorption cross sections integrated over the excitation energy. These quantities have been calculated within the framework of the recently developed unitary isobar model for pion photo- and electroproduction on the proton, which describes the available experimental data up to an excitation energy of about 1 GeV. Our results have been compared to the predictions of chiral perturbation theory.

PACS NUMBERS: 13.60.Fz, 11.55.Fv, 14.20.Dh, 13.60.Le, 13.88.+e

KEYWORDS: Inelastic electron scattering, electroexcitation, virtual Compton scattering, nucleon polarizabilities, spin content of the nucleon

*Permanent Address: Laboratory of Theoretical Physics, JINR Dubna, Head Post Office Box 79, SU-101000 Moscow, Russia

I. INTRODUCTION

Our knowledge about the nucleon's ground state and its electroexcitation spectrum is largely due to experiments with electromagnetic probes. The response of the internal degrees of freedom of the nucleon to an external electromagnetic field can be described in terms of structure-dependent polarizabilities. For real photons, these ground-state properties and polarizabilities can be related to integrals over photoabsorption cross sections by sum rules, which are based on general principles of physics such as relativity, causality and unitarity. One of the most prominent examples is the Gerasimov-Drell-Hearn (GDH) sum rule [1], which provides an astounding relationship between the anomalous magnetic moment κ of the nucleon and the difference between photoabsorption cross sections for parallel and antiparallel alignments of the photon and nucleon helicities, $\sigma_{3/2}(\omega) - \sigma_{1/2}(\omega)$. Closely related to this sum rule is the forward spin polarizability γ , which involves an integral over the same combination of cross sections, but weighted by an additional factor of ω^{-2} [2]. Another example is Baldin's sum rule [3], which expresses the sum of the electric and magnetic polarizabilities, $\Sigma = \alpha + \beta$, by an integral over the total photoabsorption cross section, $\sigma_{tot}(\omega) = [\sigma_{3/2}(\omega) + \sigma_{1/2}(\omega)]/2$.

The use of virtual photons from electron scattering processes provides us with even more detailed information on the structure of the nucleon. In particular, as we increase the four-momentum of the virtual photon Q^2 from the real-photon point ($Q^2 = 0$) to large values of Q^2 , we can investigate the transition from the nonperturbative to the perturbative regime of quantum chromodynamics (QCD). Therefore, the generalizations of real-photon sum rules to virtual photons provide an interesting possibility to study this transition and the varying role of the relevant degrees of freedom.

The general sum rules may be defined in terms of electroproduction cross sections as

$$\Sigma(Q^2) = \frac{1}{2\pi^2} \int_{\omega_{th}}^{\infty} \frac{\sigma_T(\omega, Q^2)}{\omega^2} d\omega, \quad (1)$$

$$\gamma(Q^2) = \frac{1}{4\pi^2} \int_{\omega_{th}}^{\infty} \frac{\sigma_{1/2}(\omega, Q^2) - \sigma_{3/2}(\omega, Q^2)}{\omega^3} d\omega, \quad (2)$$

where $\omega_{th} = m_\pi + (m_\pi^2 + Q^2)/2M$ is the threshold energy in the *lab* frame, $\sigma_T(\omega, Q^2)$ the transverse cross section of unpolarized electroexcitation, and $\sigma_{3/2}(\omega, Q^2)$ and $\sigma_{1/2}(\omega, Q^2)$ are the cross sections for the scattering of polarized electrons on polarized nucleons with parallel and antiparallel alignments of the electron and nucleon helicities. In a recent contribution, Edelmann, Kaiser, Piller and Weise (EKPW) [4] have evaluated such generalized sum rules in the framework of the one-loop approximation to (relativistic) chiral perturbation theory (ChPT) [5], supplemented by tree graphs for the excitation of the $\Delta(1232)$ resonance in the relativistic Rarita-Schwinger formalism.

Unfortunately, a direct measurement of the generalized polarizabilities for $Q^2 \neq 0$ is extremely difficult if not impossible, because it requires the extraction of the two-photon exchange contribution to elastic electron-proton scattering [6], the so-called “dispersion correction”. On the other hand, the polarizabilities of the nucleon at $Q^2 = 0$ can be directly measured by Compton scattering. They appear as the leading structure-dependent effect in an expansion of the six independent Compton amplitudes for small photon energies ω . However, also real Compton scattering is not at all an easy experiment, and therefore the sum rule value of $\alpha + \beta = \Sigma(Q^2 = 0)$ provides a useful constraint to determine the electric (α) and magnetic (β) polarizabilities. At present we have only scarce experimental information on the 4 spin polarizabilities γ_1 to γ_4 , except for the sum rule prediction of the “forward spin polarizability” $\gamma_1 - \gamma_2 - 2\gamma_4 = \gamma(Q^2 = 0)$, while a complete determination of these observables will require the scattering of polarized photons off polarized protons.

Recently, there have been extensive experimental and theoretical investigations of virtual Compton scattering (VCS) by means of the reaction $e + p \rightarrow e' + p' + \gamma$. This process involves the absorption of a virtual photon and the emission of a real one. In the limit of long-wave real photons, this process can also be parametrized in terms of 6 generalized polarizabilities $P_i(Q^2)$ [7,8]. However, the reader should note that VCS is characterized by a transition from a virtual ($Q^2 > 0$) to a real ($Q^2 = 0$) photon, while in the context of our present investigation a generalized polarizability refers to the scattering of a virtual photon with the same 4-momentum transfer Q^2 in the initial and final states.

The generalized polarizabilities of Eqs. (1) and (2) are, of course, constrained by real Compton scattering at $Q^2 = 0$. Their evolution with increasing values of Q^2 is of considerable interest for our understanding of the underlying dynamics, because these polarizabilities provide severe constraints to models of the nucleon at low and moderate momentum transfer. With such a perspective, we shall apply the recently developed Unitary Isobar Model (UIM) for electroproduction [9] to investigate these sum rules in the resonance region. The UIM is based on an effective phenomenological Lagrangian for Born terms and vector meson exchange in the t channel (“background”) and the dominant resonances up to the third resonance region. For each partial wave the multipoles satisfy the constraints of gauge invariance and unitarity, and in the real photon case the results agree well with the predictions of dispersion theory [10]. The model is able to describe the correct energy dependence of the multipoles for photon energies up to $\omega \simeq 1$ GeV, and it provides a good description of all experimentally measured differential cross sections and polarization observables.

The UIM was used to calculate the spin structure functions g_1 and g_2 in the resonance region for small and intermediate momentum transfer [11]. The results agree well with the asymmetries and the spin structure functions recently measured at SLAC [12]. Moreover, the first moments of the calculated spin structure functions g_1 and g_2 fulfill the Gerasimov-Drell-Hearn and Burkhardt-Cottingham [13] sum rules within 5 to 10%. One of the striking features of the generalized GDH integral is its rapid fluctuation with Q^2 and in particular a change of sign at $Q^2 \simeq 0.5$ (GeV)², which imposes severe constraints on any model for the nucleon structure. This zero-crossing separates the region dominated by resonance-driven coherent processes from a region of essentially incoherent scattering off the nucleon’s constituents. A similar zero-crossing is predicted by ChPT for the generalized spin polarizability, $\gamma(Q^2)$ [4], while we shall show that the UIM excludes such a cross-over for $Q^2 \leq (1 \text{ GeV})^2$.

In the next section we review the basic elements of the UIM, set the notation and definitions for cross sections and generalized polarizabilities. Our results are compared with ChPT in Section III, and our conclusions are presented in Section IV. Finally, some details

of the formalism are given in the Appendix.

II. CROSS SECTIONS AND THE GENERALIZED POLARIZABILITIES

In this section we set the notation and summarize the main ingredients of the UIM [9]. Let E and E' denote the energies of the electron in the initial and final states in the *lab* frame and $Q^2 = -k^2 > 0$ the four-momentum of the virtual photon. The polarization vector of the target nucleon has the components P_z (in the direction of the three-momentum of the virtual photon \mathbf{k}) and P_x (perpendicular to \mathbf{k} , in the scattering plane of the electron and in the half-plane of the outgoing electron). The differential cross section for exclusive electroproduction is then expressed in terms of the 4 virtual photoabsorption cross sections σ_T , σ_L , σ'_{LT} and σ'_{TT} by [14]

$$\frac{d\sigma}{d\Omega dE'} = \Gamma \sigma(\omega, Q^2), \quad (3)$$

where

$$\sigma = \sigma_T + \epsilon \sigma_L + h P_x \sqrt{2\epsilon(1-\epsilon)} \sigma'_{LT} + h P_z \sqrt{1-\epsilon^2} \sigma'_{TT}, \quad (4)$$

with

$$\Gamma = \frac{\alpha}{2\pi^2} \frac{E'}{E} \frac{K}{Q^2} \frac{1}{1-\epsilon}, \quad (5)$$

the flux of the virtual photon field, ϵ the transverse photon polarization, and $\omega = E - E'$ the *lab* energy of the virtual photon. As in Ref. [9], the flux is defined by the “photon equivalent energy” $K = k_\gamma = (W^2 - M^2)/2M$, where W is the total c.m. energy and M the mass of the target nucleon. We caution the reader that this definition due to Hand [15] is not unique. In particular many authors use the definition $\tilde{K}(Q^2) = \sqrt{\omega^2 + Q^2}$, which has been originally proposed by Gilman [16]. While both definitions agree at the real photon point, where they describe the *lab* momentum of the real photon, they differ in the case of electron scattering. Since the differential cross section should be independent of the choice of K or \tilde{K} , a change

of definition leads to an additional Q^2 -dependent factor $\tilde{K}/K = \sqrt{1 + Q^2/\omega^2}/(1 - Q^2/2M\omega)$ for the virtual photon absorption cross sections of Eq. (3) and, as a consequence, to different definitions of the generalized polarizabilities of Eqs. (1) and (2).

The cross sections $\sigma_{1/2}$ and $\sigma_{3/2}$ of Eqs. (1) and (2) are related to the virtual photoabsorption cross sections σ_T and σ'_{TT} by

$$\sigma_T = \frac{1}{2}(\sigma_{3/2} + \sigma_{1/2}), \quad (6)$$

$$\sigma'_{TT} = \frac{1}{2}(\sigma_{3/2} - \sigma_{1/2}). \quad (7)$$

These cross sections can be also expressed in terms of the standard quark structure functions F_1 , g_1 and g_2 depending on the Bjorken scaling variable $x = Q^2/2M\omega$ and Q^2

$$\sigma_T = \frac{4\pi^2\alpha}{MK} F_1, \quad \sigma'_{TT} = -\frac{4\pi^2\alpha}{MK} (g_1 - \frac{Q^2}{\omega^2} g_2). \quad (8)$$

Consequently, the generalized polarizabilities Σ and γ defined by Eqs. (1) and (2) can also be written in the form

$$\Sigma(Q^2) = \frac{8\alpha M}{Q^4} \int_0^{x_0} \frac{x}{1-x} F_1(x, Q^2) dx, \quad (9)$$

$$\gamma(Q^2) = \frac{16\alpha M^2}{Q^6} \int_0^{x_0} \frac{x^2}{1-x} [g_1(x, Q^2) - \frac{Q^2}{\omega^2} g_2(x, Q^2)] dx, \quad (10)$$

where $x_0 = Q^2/(2Mm_\pi + m_\pi^2 + Q^2)$ refers to the inelastic threshold of one-pion production.

Note that in the scaling regime the structure functions should depend on x only.

In our previous work [11] we generalized the GDH and BC sum rules as the first moments of the g_1 and g_2 structure functions, respectively, i.e by the integrals $I_{1(2)}(Q^2) = (2M/Q^2) \int g_{1(2)}(x, Q^2) dx$. We found that in the resonance region ($W < 2$ GeV) and for small Q^2 , the single pion production gives the dominant contribution to these integrals. However, for increasing values of Q^2 , the role of the η and multipion production channels become important. In the present paper we include these channels as well, following the procedure of Ref. [11].

The dominant contributions to the $\sigma_{1/2}$ and $\sigma_{3/2}$ cross sections, related to the single pion electroproduction, can be obtained by numerical integration of the corresponding differential cross sections, which are expressed in terms of the standard CGLN amplitudes F_1, \dots, F_4 [9]. In the UIM these amplitudes receive contributions from Born terms, including vector meson exchange, and nucleon resonances with large photon couplings up to the third resonance region, i.e. the resonances $P_{33}(1232)$, $P_{11}(1440)$, $D_{13}(1520)$, $S_{11}(1535)$, $F_{15}(1680)$, and $D_{33}(1700)$. The expressions for the cross sections $\sigma_{1/2}$ and $\sigma_{3/2}$ in terms of the CGLN amplitudes are given in the Appendix.

III. RESULTS AND DISCUSSIONS

Table I presents the separate contributions of the model ingredients to the polarizabilities Σ and γ of proton and neutron at the real photon point. The contribution of the dressed $\Delta(1232)$ excitation and its interference with the Born plus ω plus ρ (background) terms are denoted by “ Δ ”. The column “ P_{11}, D_{13}, \dots ” gives the contribution of all resonances above the $\Delta(1232)$ and their interference with the background and the $\Delta(1232)$, and so forth for the columns labeled η and multipion. Finally, the sum of all contributions is contained in the column “total” of the table.

Our results for $\alpha + \beta$ agree well with the existing analysis of the sum rules (see, e.g., Ref. [17] for a review),

$$\alpha^p + \beta^p \simeq (14.3 \pm 0.5) \times 10^{-4} \text{fm}^3, \quad (11)$$

$$\alpha^n + \beta^n \simeq (15.8 \pm 0.5) \times 10^{-4} \text{fm}^3. \quad (12)$$

In a more recent evaluation of the sum rule, Babusci et al. [18] found somewhat reduced values, $\alpha^p + \beta^p = 13.69 \pm 0.14$ and $\alpha^n + \beta^n = 14.40 \pm 0.66$ in units of 10^{-4}fm^3 . Part of the deviations might be attributed to the contribution of the deep inelastic domain, which is included in the calculation of Ref. [18] but not in our result. We also found a discrepancy of about 10% in the numerical calculation of the dispersion integral in the threshold region

($\omega_{thr} \leq \omega \leq 0.2$ GeV). Using the same set of pion photoproduction multipoles of Ref. [18], we obtained $(\alpha + \beta)_p^{thr} = 1.14$ and $(\alpha + \beta)_n^{thr} = 1.70$ instead of $(\alpha + \beta)_p^{thr} = 1.25$ and $(\alpha + \beta)_n^{thr} = 1.86$ as quoted in Ref. [18].

As may be seen from Table I, the Born terms are by far the major contributor to $\alpha + \beta$, followed by the $\Delta(1232)$ resonance and multipion production. Our total values for Σ^p and Σ^n are similar to those obtained within relativistic ChPT [4],

$$\Sigma_{\text{ChPT}}^p(0) = (5.48 + 8.23) \times 10^{-4} \text{ fm}^3 = 13.71 \times 10^{-4} \text{ fm}^3, \quad (13)$$

$$\Sigma_{\text{ChPT}}^n(0) = (8.90 + 8.23) \times 10^{-4} \text{ fm}^3 = 17.13 \times 10^{-4} \text{ fm}^3, \quad (14)$$

with the two terms in the central part of this equation giving the individual contributions of pion-loop and Δ -pole terms. Regarding these individual contributions, however, our results differ considerably. In particular in the case of the proton, our background contribution is 50 % larger than the pion-loop contribution of Ref. [4], and our Δ contribution is only 25 % of the value of that reference. In fact we also find a large value for the $\Delta(1232)$ alone, $\Sigma_\Delta^p = 9.8 \times 10^{-4} \text{ fm}^3$ (see Fig. 4(c)). However, the interference with the background reduces this value to $2.04 \times 10^{-4} \text{ fm}^3$ (see Table I).

In the case of the spin polarizability γ , there also occurs a big cancellation between the “background” (essentially S-wave pion production near threshold) and the $\Delta(1232)$, while all other contributions are found to be extremely small, because of the damping factor $1/\omega^3$ in the integrand of Eq. (2). In the neutron channel, this cancellation is almost complete and γ_n is practically zero. Due to the $1/\omega^3$ damping factor we expect the contributions of the deep inelastic region to be small as well.

As in the case of the GDH sum rule, the spin polarizability γ is very sensitive to an exact treatment of the E_{0+} photoproduction multipole in the threshold region [19,20]. Moreover, the value of γ is almost entirely given by the contributions of the multipoles E_{0+} and M_{1+} , which contribute with opposite signs. The predicted values of the UIM,

$$\gamma^p \simeq -0.6 \times 10^{-4} \text{ fm}^4, \quad (15)$$

$$\gamma^n \simeq 0 \times 10^{-4} \text{ fm}^4, \quad (16)$$

are much smaller (in absolute value) than the ones obtained from the SAID multipoles [21,22], and relativistic chiral perturbation theory [4,5]. We note, however, that the results of relativistic ChPT [5] are not based on a systematic expansion in $1/M$.

We also point out that our value for γ^p carries a sign opposite to the prediction of heavy baryon ChPT [23]. This is a rather intriguing result, since this theory does indeed provide a systematic expansion in $1/M$. Similarly as in the case of $\alpha+\beta$, for which the theory obtains a much too large value, the reason for this shortcoming might be due to large loop corrections in fourth order (ϵ^4), which have been neglected in the ϵ^3 approximation of Ref. [23]. We further record that a recent calculation based on the Chiral Soliton Model [24] predicted $\gamma^p = \gamma^n = -0.1 \times 10^{-4} \text{ fm}^4$.

The values for the spin polarizabilities predicted from the UIM are in good agreement with the results of Refs. [19,25], obtained on the basis of the HDT multipoles [10]. These multipoles are generated by dispersion relations at fixed t , and they provide an excellent description of the photoproduction data for $\omega \leq 450 \text{ MeV}$ [26]. In particular, these multipoles are also in agreement with the low energy theorems [5].

Next, we present our results for the generalized polarizabilities. In Fig. 1, we show the evolution of $\Sigma(Q^2)$ for (a) the proton and (b) the neutron. Clearly seen in the figure are the large individual contributions of the Born terms and of the $\Delta(1232)$. It should also be noted that the contribution of multipion production can not be neglected.

Fig. 2 shows our predictions for $\gamma(Q^2)$ for (a) the proton and (b) the neutron. As in the case of real photons, the main contributions are from the Born terms and the $\Delta(1232)$, and there occur large cancellations between these two contributions. The higher resonances as well as η and multipion production are quite negligible due to the weighting factor ω^{-3} in the integrand.

In Fig. 3 we compare the predictions of the UIM (solid lines) and relativistic ChPT (dashed lines) for the generalized polarizabilities. As can be seen, there are significant, qualitative and quantitative, differences between the UIM and ChPT predictions. The most striking difference refers to the slope of the $\gamma(Q^2)$ close to the real photon point. With

increasing values of Q^2 , the UIM prediction for the background drops much faster than the $\Delta(1232)$ contribution, and as a result a steep slope develops for $Q^2 < 0.1 \text{ (GeV)}^2$. Relativistic ChPT on the other hand, predicts a rather flat behavior in this region. The pronounced slope in $\gamma(Q^2)$ observed in the UIM is due to the interference between background and $\Delta(1232)$ terms, as we shall explain later.

In Fig. 4, we show the individual contributions of the background (dotted lines), the $\Delta(1232)$ *only* (dashed lines), and the interference between background and $\Delta(1232)$ (dash-dotted lines). The sum of these three contributions is given by the solid line. The big destructive interference between background and $\Delta(1232)$ contributions to $\Sigma(Q^2)$ and $\gamma(Q^2)$ is now immediately visible, and the pronounced slope of $\gamma(Q^2)$ near the origin is seen to result from the interference term.

It is interesting that we do not find a zero-crossing for $\gamma^p(Q^2)$ and $\gamma^n(Q^2)$ in the range of $Q^2 \leq 1.0 \text{ (GeV)}^2$, while Ref. [4] predicts such a crossing at $Q^2 \sim 0.4 \text{ (GeV)}^2$. In our previous work [11], we found that the UIM gives a zero-crossing at $Q^2 \sim 0.5 \text{ (GeV)}^2$ for the GDH integral I_1 which is similar to γ but with a weighting factor ω^{-1} in the integrand and an extra term proportional to σ'_{LT} (whose contribution is small for $Q^2 \sim 0.5 \text{ (GeV)}^2$). The origin of this phenomenon is the cancellation between the (negative) contribution from the Δ resonance and the (positive) contributions from the higher resonances and η plus multipion channels. The contribution of the η plus multipion channels becomes more and more important with increasing Q^2 , with the eventual result of a positive value for the GDH integral. However, as we have pointed out before, the η plus multipion channels are more strongly suppressed in the case of γ than for the GDH integral. Therefore, the zero crossing of γ does not appear at low values of Q^2 . Numerically we find that γ^p changes sign at $Q^2 \sim 1.4 \text{ (GeV)}^2$, and γ^n at $Q^2 \sim 2 \text{ (GeV)}^2$.

As a final remark, we mention that the discussed interference between background and $\Delta(1232)$ terms originates from the *dynamical* dressing of the $\gamma N \Delta$ vertex, which is pictorially shown in Fig. 5. The main mechanism to renormalize the $\gamma N \Delta$ vertex is diagram 5(b), because this diagram has a strong imaginary part. As is obvious from the optical theorem,

this imaginary part individually leads to a strong interference term. In our calculation of pion production such contributions appear naturally in the expressions for the differential cross sections.

IV. CONCLUSION

We evaluated the generalized Baldin sum rule $\Sigma(Q^2)$ and the spin polarizability $\gamma(Q^2)$ for small and moderate values of Q^2 using the Unitary Isobar Model (UIM) [9]. Both $\Sigma(Q^2)$ and $\gamma(Q^2)$ are dominated by background and $\Delta(1232)$ resonance contributions. In addition $\Sigma(Q^2)$ also receives sizable contributions from multipion processes.

Our predictions were compared with a recent calculation in the framework of relativistic chiral perturbation theory (ChPT). While the total value of Σ agrees well with the result of ChPT and other phenomenological calculations, we differ from ChPT in the case of $\gamma(0)$. Although one has to recognize that the predictions of relativistic ChPT are not based on a consistent $1/M$ expansion, the agreement with the phenomenological result based on the SAID multipoles SP97K, has been taken as some assurance of the convergence of the expansion. However, as was remarked earlier [19,20], these SAID multipoles did not describe the threshold dependence of the E_{0+} photoproduction multipole but were at variance with the low energy theorems. We repeat that the correct threshold behavior of the multipole E_{0+} is extremely important for both γ and the closely related GDH sum rule.

We also found significant, qualitative and quantitative, differences between the UIM and ChPT predictions for the evolution of Σ and γ with momentum transfer. The most important qualitative difference concerns the absence of the interference between background and $\Delta(1232)$ resonance in Ref. [4]. While this interference does not lead to big effects for the net value of $\Sigma(Q^2)$, it has a dramatic effect for $\gamma(Q^2)$, in particular for $Q^2 < 0.1 \text{ (GeV)}^2$. The physical origin for the interference is the dynamical dressing of the $\gamma N \Delta$ vertex [27].

We are looking forward to experimental tests of our predictions by polarized electroproduction cross sections, which will become available in the near future. There are indeed

quite a few proposals in several laboratories throughout the world to perform such experiments, e.g. at Jefferson Lab, ELSA and MAMI. The experimental data presently available do not allow a very precise determination of many ingredients of the UIM. Among the most important ones, is the relative contribution of background and resonances to the multipoles. While the pseudovector Born terms are well described, additional background contributions are model dependent, such as loop effects, pion rescattering or u-channel resonances. The common feature of such effects is that they are weakly energy dependent and visible mostly in S waves. As far as the existing data are concerned, they are well described by the UIM, which is constrained by unitarity and gauge invariance. Therefore, the UIM should provide a reasonable first estimate for the sum rules. Of course, it is only with the availability of new experimental data in the near future that models like the UIM can be firmly tested. Such data will certainly enhance our knowledge on various aspects of nonperturbative QCD in general and, in particular, on the low energy spin structure of the nucleon.

ACKNOWLEDGMENTS

This work has been supported in part by Deutsche Forschungsgemeinschaft, SFB 443 (Germany) and by CNPq (Brazil).

APPENDIX:

In this appendix we give the expressions of the single-pion electroproduction cross sections $\sigma_{1/2}$, $\sigma_{3/2}$ and σ'_{LT} in terms of the standard CGLN amplitudes F_1, \dots, F_6 . The definition of these amplitudes is the same as in Ref. [9]. Within the UIM, they can be calculated using the on-line version of the numerical program MAID accessible on the internet by <http://www.kph.uni-mainz.de/T/maid/>.

The expressions for the cross sections are greatly simplified by introducing the spin amplitudes $\mathcal{H}_1, \dots, \mathcal{H}_6$ [28]

$$\mathcal{H}_1 = \frac{-\sin \theta_\pi}{\sqrt{2}} (F_3 + F_4 \cos \theta_\pi), \quad \mathcal{H}_2 = \frac{-1}{\sqrt{2}} (2F_1 - 2F_2 \cos \theta_\pi) + \mathcal{H}_3,$$

$$\mathcal{H}_3 = \frac{-1}{\sqrt{2}} F_4 \sin^2 \theta_\pi, \quad \mathcal{H}_4 = \frac{\sin \theta_\pi}{\sqrt{2}} (2F_2 + F_3 + F_4 \cos \theta_\pi), \quad (\text{A1})$$

$$\mathcal{H}_5 = F_5 + F_6 \cos \theta_\pi, \quad \mathcal{H}_6 = F_6 \sin \theta_\pi,$$

where θ_π is the polar angle of the outgoing pion. In terms of these spin amplitudes, the cross sections $\sigma_{1/2}$, $\sigma_{3/2}$ and σ'_{LT} are given by

$$\sigma_{1/2} = \frac{q}{k_\gamma^{cm}} \int d\Omega_\pi (|\mathcal{H}_2|^2 + |\mathcal{H}_4|^2), \quad (\text{A2})$$

$$\sigma_{3/2} = \frac{q}{k_\gamma^{cm}} \int d\Omega_\pi (|\mathcal{H}_1|^2 + |\mathcal{H}_3|^2), \quad (\text{A3})$$

$$\sigma'_{LT} = \frac{q}{k_\gamma^{cm}} \frac{Q}{\omega^{cm}} \int d\Omega_\pi \frac{1}{\sqrt{2}} \text{Re}(\mathcal{H}_5 \mathcal{H}_2^* + \mathcal{H}_6 \mathcal{H}_4^*), \quad (\text{A4})$$

where $q = |\mathbf{q}|$ and $\omega^{cm} = (W^2 - M^2 - Q^2)/2W$ are the pion momentum and the virtual photon energy respectively, in the c.m. frame. The “photon equivalent energy” in the c.m. frame is defined as $k_\gamma^{cm} = (W^2 - M^2)/2W$. Note that in comparison with the standard nomenclature of deep inelastic scattering (DIS) [12], our interference cross sections are $\sigma'_{LT} = -\sigma_{LT}(\text{DIS})$ and $\sigma'_{TT} = -\sigma_{TT}(\text{DIS}) = (\sigma_{3/2} - \sigma_{1/2})/2$.

REFERENCES

- [1] S.B. Gerasimov, Sov. J. Nucl. Phys. 2 (1966) 430; S.D. Drell and A.C. Hearn, Phys. Rev. Lett. 16 (1966) 908.
- [2] M. Gell-Mann, M. Goldberger and W. Thirring, Phys. Rev. 95 (1954) 1612.
- [3] A.M. Baldin, Nucl. Phys. 18 (1960) 310.
- [4] J. Edelmann, N. Kaiser, G. Piller and W. Weise, Nucl. Phys. A 641 (1998) 119.
- [5] V. Bernard, N. Kaiser and U.-G. Meissner, Nucl. Phys. B 373 (1992) 346; V. Bernard, N. Kaiser J. Kambor and U.-G. Meissner, Nucl. Phys. B 388 (1992) 315; V. Bernard, N. Kaiser, U.-G. Meissner and A. Schmidt, Phys. Lett. B 319 (1993) 269 and Z. Phys. A 348 (1994) 317.
- [6] S.D. Drell and M.A. Ruderman, Phys. Rev. 106 (1957) 561.
- [7] P. A. M. Guichon, G. Q. Liu and A.W. Thomas, Nucl. Phys. A 591 (1995) 606; P.A.M. Guichon and M. Vanderhaeghen, Prog. Part. Nucl. Phys. 41 (1998) 125.
- [8] D. Drechsel, G. Knöchlein, A.Yu. Korchin, A. Metz and S. Scherer, Phys. Rev. C 57 (1998) 941; *ibid* Phys. Rev. C 58 (1998) 1751.
- [9] D. Drechsel, O. Hanstein, S.S. Kamalov and L. Tiator, Nucl. Phys. A 645 (1999) 145.
- [10] O. Hanstein, D. Drechsel and L. Tiator, Nucl. Phys. A 632 (1998) 561.
- [11] D. Drechsel, S.S. Kamalov, G. Krein and L. Tiator, Phys. Rev. D 59 (1999) 094021.
- [12] E143 Collaboration, K. Abe et al., Phys. Rev. Lett. 78 (1997) 815.
- [13] H. Burkhardt and W.N. Cottingham, Ann. Phys. (N.Y.) 56 (1970) 543.
- [14] D. Drechsel, Prog. Part. Nucl. Phys. 34 (1995) 181.
- [15] L.N. Hand, Phys. Rev. 129 (1963) 1834.

- [16] F.J. Gilman, Phys. Rev. 167 (1968) 1365.
- [17] A.I. L'vov, Int. J. Mod. Phys. 8 (1993) 5267.
- [18] D. Babusci, G. Giordano and G. Matone, Phys. Rev. C 57 (1998) 291.
- [19] D. Drechsel, G. Krein and O. Hanstein, Phys. Lett. B 420 (1998) 248.
- [20] D. Drechsel and G. Krein, Phys. Rev. D 58 (1998) 116009.
- [21] A.M. Sandorfi, C.S. Whisnant and M. Khandaker, Phys. Rev. D 50 (1994) R6681.
- [22] R.A. Arndt, I.I. Strakovsky and R.L. Workman, Phys. Rev. C 53 (1996) 430, Solution SP97K.
- [23] T.R. Hemmert, B.R. Holstein, J. Kambor and G. Knöchlein, Phys. Rev. D 57 (1998) 5746 .
- [24] Y. Tanushi, S. Saito, M. Uehara, nucl-th/9901010.
- [25] D. Drechsel, M. Gorchtein, B. Pasquini and M. Vanderhaeghen, hep-ph/9904290.
- [26] M. Fuchs et al., Phys. Lett. B 368 (1996) 20; R. Beck et al., Phys. Rev. Lett. 78 (1997) 606; F. Härter, Ph.D. Thesis, Mainz (1996).
- [27] S. S. Kamalov and S. N. Yang, “Pion cloud and the Q^2 –dependence of $\gamma^*N \leftrightarrow \Delta$ transition form factors”, nucl-th/9904072.
- [28] G. Knöchlein, D. Drechsel and L. Tiator, Z. Phys. A 352 (1995) 327.

TABLES

TABLE I. Contributions to $\Sigma(0) = \alpha + \beta$ (in units of 10^{-4} fm^3) and $\gamma(0) = \gamma$ (in units of 10^{-4} fm^4) for proton and neutron. For details see text.

	Born+ $\omega + \rho$	Δ	P_{11}, D_{13}, \dots	η	multipion	total
$\alpha^p + \beta^p$	9.17	2.04	0.56	0.08	1.56	13.41
γ^p	0.90	-1.51	-0.03	0.02	-0.03	-0.65
$\alpha^n + \beta^n$	10.86	2.04	0.45	0.08	1.56	14.99
γ^n	1.54	-1.51	0.06	0.02	-0.03	0.08

FIGURES

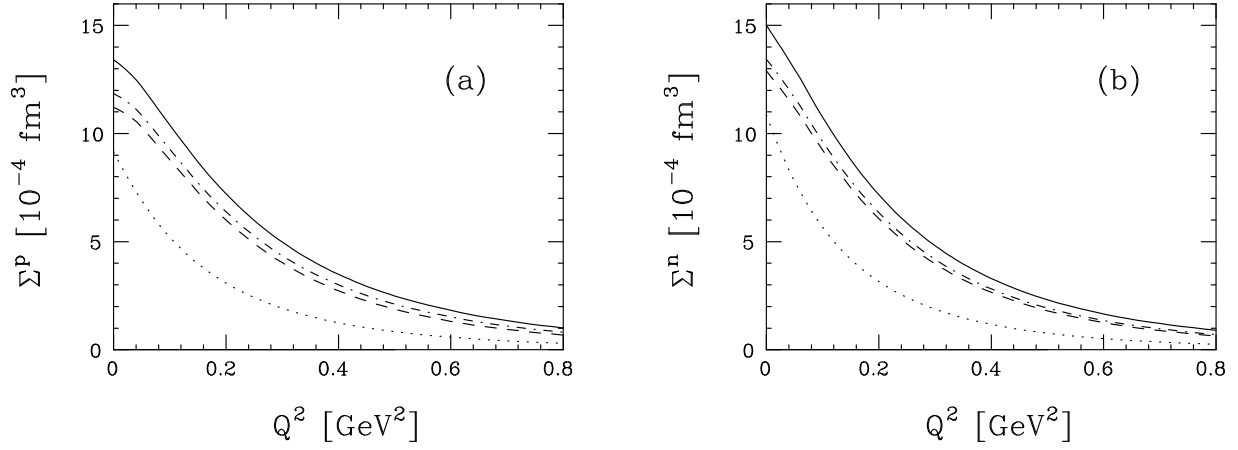


FIG. 1. The sum of the electric and magnetic polarizabilities of (a) proton and (b) neutron as function of Q^2 . The solid line is the full result including the 1π , η and $n\pi$ contributions. The dotted line represents the contribution of Born terms and vector mesons. The dashed line is obtained by adding the $\Delta(1232)$ resonance, and the dash-dotted line by adding all resonances and the η channel. The difference between the full and the dash-dotted lines is therefore due to the production of two and more pions.

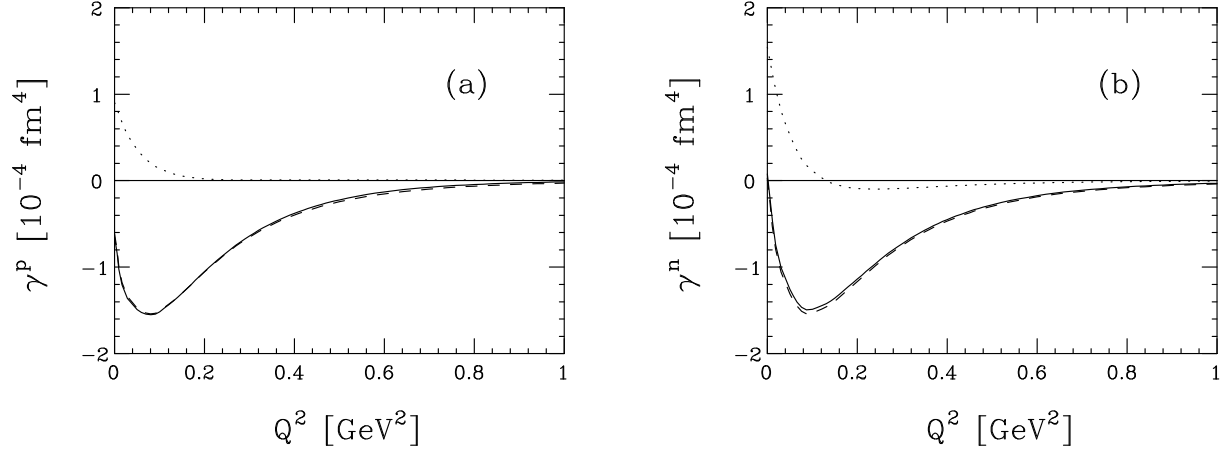


FIG. 2. The generalized spin polarizability of (a) proton and (b) neutron as function of Q^2 . The dotted line represents the contributions of Born terms and vector mesons, the dashed line includes both the Born terms and the $\Delta(1232)$. The solid line (almost on top of the dashed line) also includes the higher resonances as well as η and multipion production.

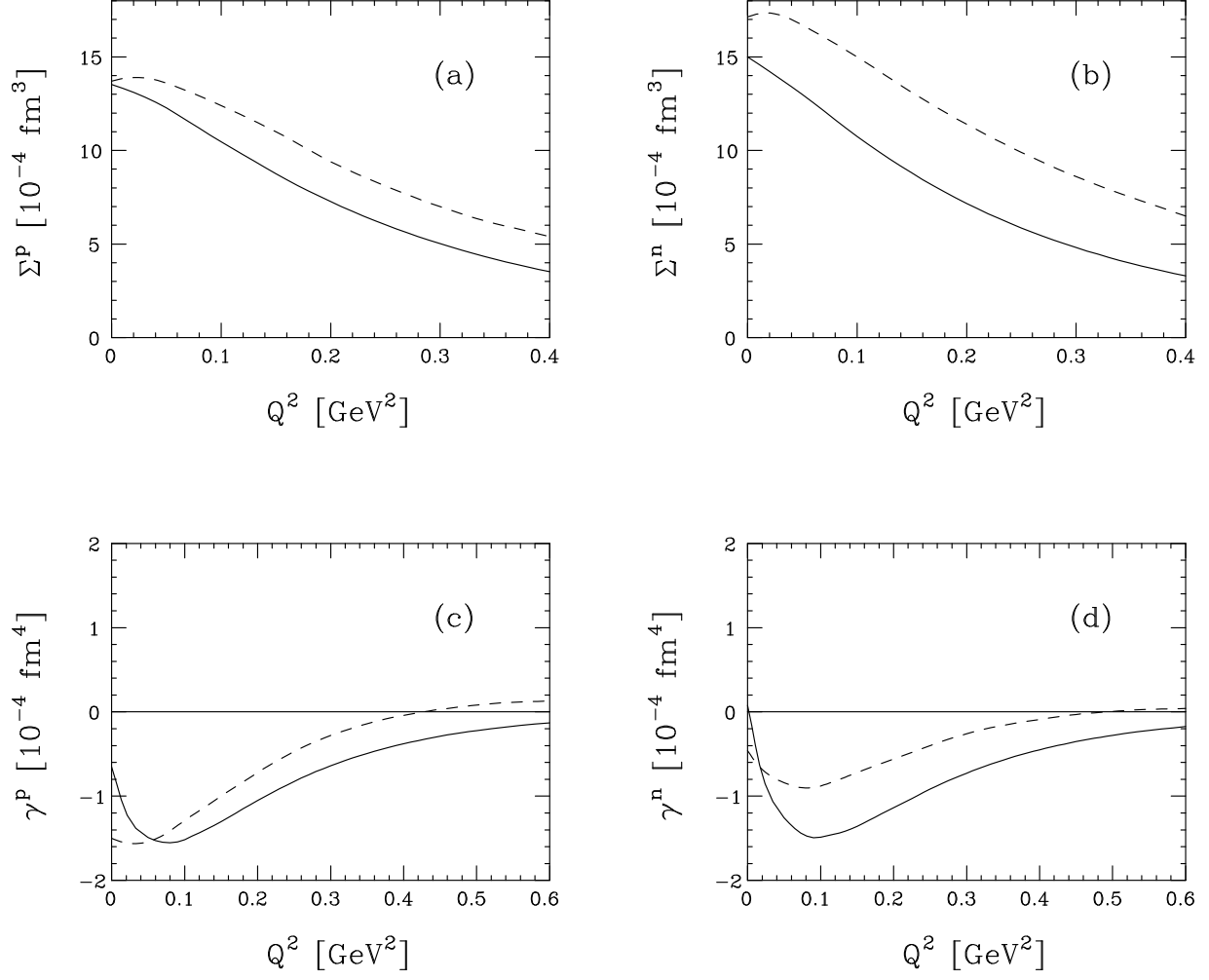


FIG. 3. Comparison of the UIM (solid) and ChPT results (dashed).

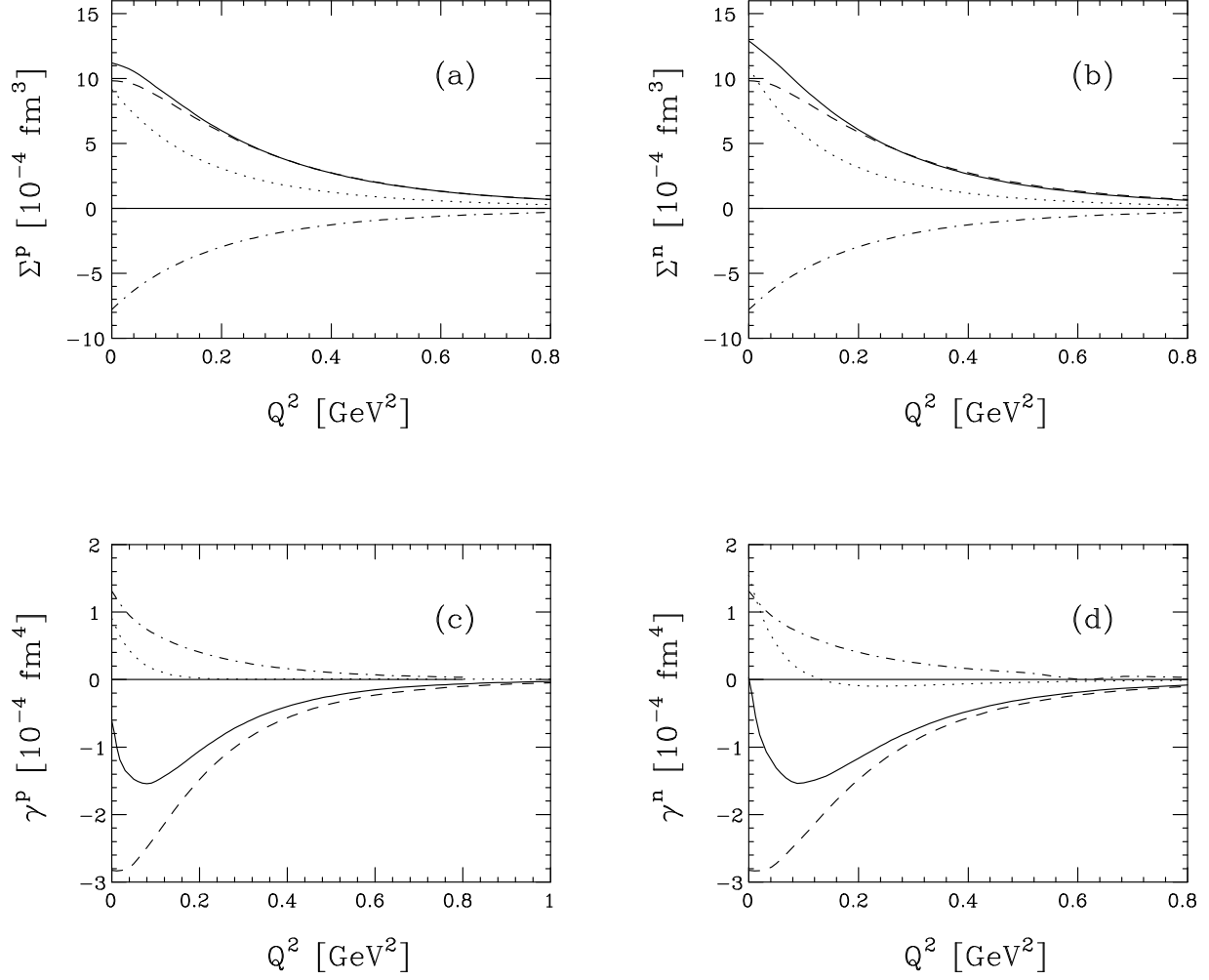


FIG. 4. Contributions to $\Sigma(Q^2)$ and $\gamma(Q^2)$ from the background (dotted lines) and the $\Delta(1232)$ only (dashed lines). The interference between the background and the Δ is shown in the dot-dashed line. The solid line is the sum of the three contributions.

$$\text{Im} \left\{ \text{---} \text{---} \text{---} \right\} \approx \text{---} \text{---} \text{---} + 2 \text{---} \text{---} \text{---}$$

$v_{\gamma\pi}^{\Delta}$ $v_{\pi\gamma}^{\Delta}$ a) $v_{\gamma\pi}^{\Delta}$ $v_{\pi\gamma}^B$ b)

FIG. 5. Pictorial representation of the $\Delta(1232)$ contribution to the imaginary part of the Compton scattering amplitude in one pion loop approximation. Diagram (b) leads to the interference of the background with the $\Delta(1232)$, where $v_{\pi\gamma}^{\Delta}$ and $v_{\pi\gamma}^B$ represent respectively the Δ -pole and background amplitudes.